# A universal law for capillary rise in corners

Alexandre Ponomarenko, David Quéré, Christophe Clanet

*J. Fluid Mech.* (2011), *vol.* 666, *pp.* 146–154. 
doi:10.1017/S0022112010005276

# A universal law for capillary rise in corners

ALEXANDRE PONOMARENKO, DAVID QUÉRÉ AND CHRISTOPHE CLANET†

PMMH (Physique et Mécanique des Milieux Hétérogènes), UMR7636 du CNRS, ESPCI, 10 rue Vauquelin, 75005 Paris, and LadHyX, UMR7646 du CNRS, Ecole Polytechnique, 91128 Palaiseau, France

(Received 30 July 2010; revised 29 September 2010; accepted 29 September 2010)

We study the capillary rise of wetting liquids in the corners of different geometries and show that the meniscus rises without limit following the universal law: $h(t)/a \approx (\gamma t/\eta a)^{1/3}$, where $\gamma$ and $\eta$ stand for the surface tension and viscosity of the liquid while $a = \sqrt{\gamma/\rho g}$ is the capillary length, based on the liquid density $\rho$ and gravity $g$. This law is universal in the sense that it does not depend on the geometry of the corner.

**Key words:** capillary flows, porous media

## 1. Introduction

According to Hardy (1922), the study of surface energies and short-range forces started with Boyle's experiment on capillary rise in 1682 (Boyle 1682). This experiment consists in contacting a wetting liquid with a vertical tube. The liquid spontaneously rises up to a final height $h_e$, whose value is inversely proportional to the tube radius $r$ ($h_e \sim 1/r$). The interest of physicists, or even physicians, for capillary rise is naively explained in the *Encyclopedia Diderot d'Alembert*, first published in 1751: *The spontaneous rise of water in a capillary tube, which seems to contradict the law of gravitation, deserves our attention. Indeed, the human body is a hydraulic machine where the number of capillary tubes is almost infinite.*

Following more than one century of experiments, the theory of capillary rise was proposed by Laplace (1806), who determined in particular the final height of rise:

$$\frac{h_e}{r} = 2\left(\frac{a}{r}\right)^2 \cos\theta. \tag{1.1}$$

In this expression, $a = \sqrt{\gamma/\rho g}$ is the capillary length and $\theta$ is the contact angle that characterizes the wetting of the liquid on the solid ($\theta = 0$ in the limit of complete wetting). In the expression of the capillary length, $\gamma$, $\rho$, $g$ respectively stand for surface tension, liquid density and gravity. The law (1.1) is often referred to as Jurin's law, following the work of Jurin (1718). It reveals that the capillary rise becomes significant only in tubes of diameter smaller than the capillary length (millimetric). It also predicts a height of 30 km for nanopores ($r = 0.5$ nm). The question of the maximum possible value of $h_e$ has recently been addressed by Caupin *et al.* (2008).

† Email address for correspondence: clanet@ladhyx.polytechnique.fr

It took another century to solve the question of the dynamics $h(t)$ of the rise. The solution was found by Lucas (1918) and independently, in the context of oil extraction, by Washburn (1921). They both showed that for a liquid of viscosity $\eta$ in a horizontal tube, the meniscus moves according to the law:

$$h(t) = \sqrt{\mathscr{D}t} \quad \text{with} \quad \mathscr{D} = 2\frac{\gamma r \cos\theta}{\eta}. \tag{1.2}$$

For a vertical tube, this law holds in the limit $h \ll h_e$, where gravity can be neglected. The major assumption used in (1.2) is the constancy of the contact angle $\theta$. The studies of dynamical wetting (Hoffman 1974; Tanner 1979; de Gennes 1985) later showed that this is generally not the case, so that the Lucas–Washburn law must be corrected in the first steps of the rise (Siebold 2000; Wolf 2010). Another assumption in this law is that inertia is negligible. When this approximation is not satisfied, Quéré (1997) and Quéré, Raphael & Ollitrault (1999) reported a very different behaviour for the rise, composed of an initial phase of constant velocity followed by oscillations around the equilibrium $h = h_e$. The transition from the viscous to the inertial regime was discussed by Fries & Dreyer (2008).

On the applied side, capillary rise plays a major role in the imbibition of porous media (Kistler 1993; Steen 1996; Lago & Araujo 2001; Marmur 2003). Its main applications are, among others, in soil imbibition (Depountis *et al.* 2001; Ramrez-Flores, Bachmann & Marmur 2010), wicking in textiles (Ferrero 2003), flows in foams (Caps *et al.* 2005) or powders (Galet, Patry & Dodds 2010) and civil engineering materials (Karoglou *et al.* 2005; Hall & Hoff 2007). In all these examples, the geometry of the porous media is far from a collection of cylindrical tubes and the applicability of Jurin's and Lucas–Washburn's laws can be questioned (van Brakel & Heertjes 1975; Lago & Araujo 2001). This led to the study of capillary rise in more complex geometries, such as between cylinders (Princen 1968, 1969), in rectangular tubes (Ramos & Cerro 1994; Weislogel & Lichter 1998; Bico & Qur 2002), or on textured surfaces (Ishino *et al.* 2007). For each of these systems, the wicking process is characterized by well-defined length scales (distance between the cylinders for Princen, or size of the rectangular cavities for examples).

Our aim in this study is to characterize capillary rise in 'open' geometries, which do not impose any length scale. Two of these geometries are sketched in figure 1(*a*, *b*). The linear case (figure 1*a*) has been studied by Higuera, Medina & Linan (2008) in the limit of small angles ($\alpha = 0.75^\circ$). Using the lubrication approximation, these authors found a self-similar solution, with a $t^{1/3}$ time evolution for the liquid front, compatible with the theory of Tang & Tang (1994). After presenting the experimental set-up and results, we will compare the data obtained in linear (figure 1*a*), quadratic (figure 1*b*) and cubic corners (figure 4*a*,*b*) with the small-angle limit and discuss the general properties of capillary rise in corners.

## 2. Experimental set-up and protocol

The experimental set-up used to study capillary rise in a quadratic corner is shown in figure 1(*c*). Two solid rods made of Plexiglas are pressed together by regularly spaced threaded rods. The diameter $D$ of the cylinders is varied from 10 to 30 mm. The wetting liquid is a silicon oil ($\gamma = 20$ mN m$^{-1}$) of viscosity $\eta$ between 10 and 1000 mPa s. The liquid is contained in a Petri dish whose vertical position is controlled by a Micro-Controle translation table. This yields a precise and reproducible contact. The capillary rise of the liquid in the corner is observed through the cylinders

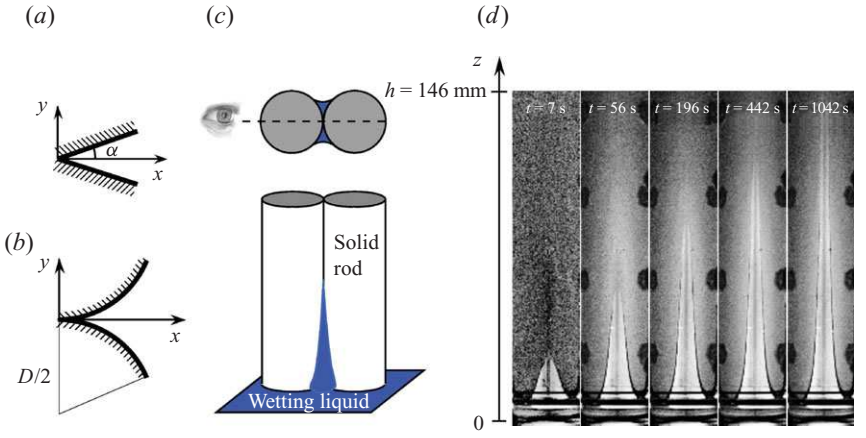


FIGURE 1. (Colour online) (*a*) Linear corner $y = \tan\alpha x$. (*b*) Quadratic corner $y = x^2/D$. (*c*) Sketch of the experiment. (*d*) Typical sequence obtained with solid rods made of Plexiglas (diameter $D = 30\,\text{mm}$) and brought in contact with a silicone oil V20 ($\eta = 20\text{mPa s}$, $\gamma = 20\text{mN m}^{-1}$).

(figure 1*c*) via a D300 Nikon programmable camera. The location of the front is determined by subtracting, from each image, the initial unwetted reference frame. An example of the rise is shown in figure 1(*d*), where the wetted region appears in light grey and the determination of the liquid front $h(t)$ does not present any ambiguity. The actual shape of the wetted area is more difficult to extract from these pictures since the observation is made through cylindrical Plexiglas lenses. In this study, we focus on the time evolution $h(t)$ of the liquid height.

## 3. Experimental results

In the sequence 1(*d*) it can be seen that the front progresses in a strongly nonlinear fashion. It takes 196 s to reach 73 mm and 1042 s to double this distance. More quantitatively, the height $h(t)$ is shown in figure 2. For different cylinder diameters, figure 2(*a*) shows the front dynamics obtained with silicone oil 10 times more viscous than water. After an initial phase of about 10 s, the front progresses as $t^{1/3}$. This evolution does not depend on the rod diameter. For a fixed diameter $D = 30\,\text{mm}$, the influence of the viscosity on the capillary rise can be seen in figure 2(*b*): the larger the viscosity, the longer the time needed to reach a given height. As an example, it takes 100 s to reach 100 mm with a silicon oil V10, whereas an oil 100 times more viscous reaches the same height in $10^4$ s, suggesting a characteristic time of rise proportional to $\eta$. For all the viscosities, the rise comprises an initial 'quick' rise followed by a $t^{1/3}$ evolution. The duration of the initial regime also increases with the viscosity.

## 4. The organ model

Figure 3(*a*) shows a sketch of our model to capture the dynamics of the rise. For a corner of arbitrary shape, we model it as a kind of organ, that is, a collection of juxtaposed tubes of decreasing diameters as they approach the corner. Our main assumptions here are that the motion is mainly vertical and that the curvature imposed by the wall confinement (in the $(y, z)$-plane) dominates the curvature in the $(x, z)$-plane, as indicated by the observations of the wetting front (figure 1*d*).

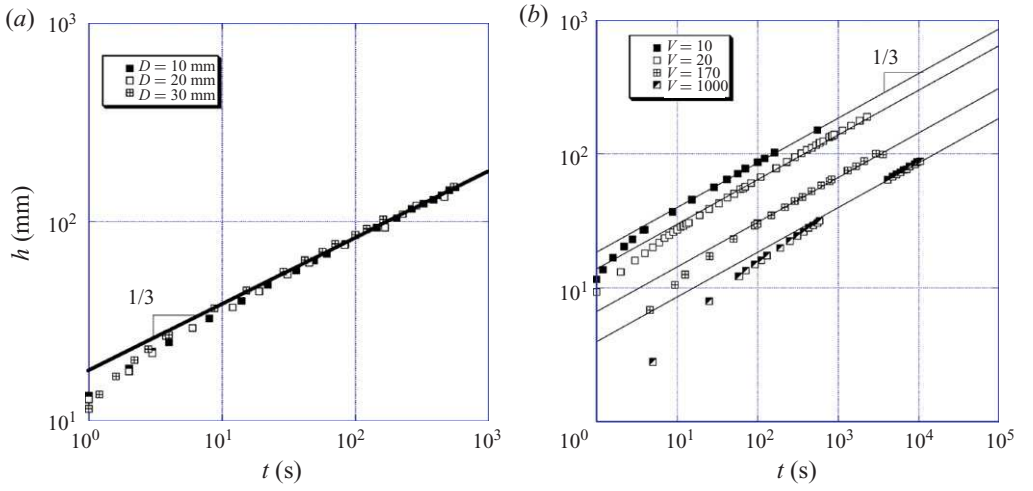


FIGURE 2. (Colour online) Experimental results for the time evolution of the position of the liquid front. (*a*) The wetting liquid is a silicon oil (viscosity $\eta = 10$ mPa s, surface tension $\gamma = 20$ mN m$^{-1}$) and the diameter of the solid rods is changed. (*b*) The diameter of the plain cylinders is kept constant ($D = 30$ mm) but the silicon oil viscosity $\eta$ is varied between 10 and 1000 mPa s. The solid lines indicate the slope 1/3.

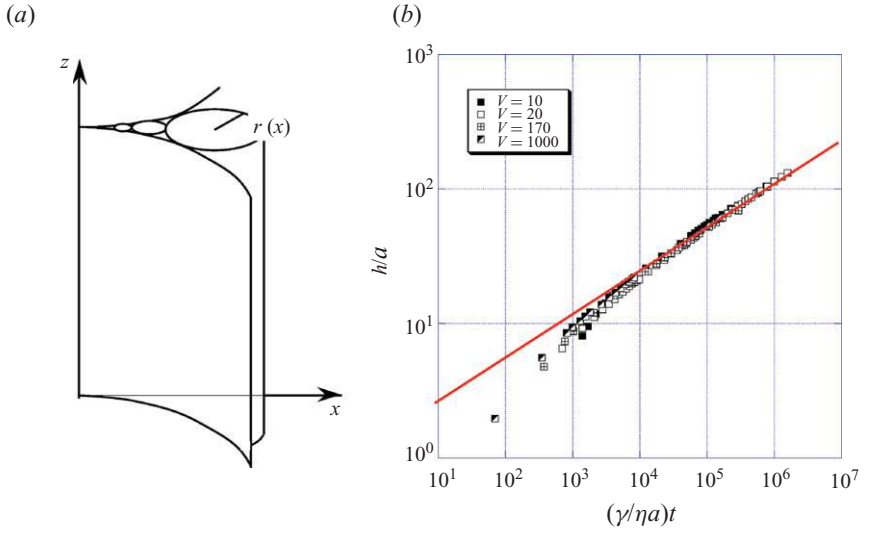


FIGURE 3. (Colour online) (*a*) Presentation of the 'organ' model. (*b*) Evolution of the normalized height $h/a$ as a function of the reduced time $(\gamma/\eta a)t$. The solid line shows the slope 1/3 (4.4).

As the corner contacts the wetting liquid, the rise starts in the collection of juxtaposed tubes and we try to understand the race between the menisci in each tube. By definition, the height of the leader, which is not always in the same tube, is $h(t)$. If $h_r(r, t)$ stands for the location of the front in the tube of radius $r$ at time $t$, Stokes'

equation can be written in the scaling form:

$$\frac{\gamma}{rh_r} \sim \rho g + \eta \frac{\dot{h}_r}{r^2}. \tag{4.1}$$

Equation (4.1) shows that the driving capillary pressure gradient $\gamma/rh_r$ is balanced by both the force of gravity $\rho g$, and the viscous friction based on the velocity of the front $\dot{h}_r$. This classical equation can be integrated as

$$h_r(r,t) \sim \sqrt{\frac{2\gamma r}{\eta}t} - \frac{\rho g r^2}{\eta}t. \tag{4.2}$$

At short times, gravity can be neglected and we recover the Lucas–Washburn behaviour. More generally, (4.2) provides the radius $r_L$ of the leading meniscus, deduced from the condition $(\partial h_r/\partial r)_{r=r_L} = 0$. Hence, we find

$$r_L \sim \left(\frac{1}{8}\frac{\eta\gamma}{\rho^2 g^2 t}\right)^{1/3}. \tag{4.3}$$

The position of the front thus approaches the corner as $1/t^{1/3}$. Since our definition of $h(t)$ is $h_r(r_L, t)$, we can deduce from (4.2) and (4.3) the dynamics of the capillary rise:

$$h(t) \sim \left(\frac{\gamma^2 t}{\eta\rho g}\right)^{1/3}. \tag{4.4}$$

This scaling law is in good agreement with the experimental observations reported in figure 2. The capillary rise does not depend on the rod diameter $D$. Moreover, the time needed to reach a fixed height is proportional to the viscosity. Finally, the model predicts the $t^{1/3}$ behaviour observed at long times. Rewriting (4.4) as $h/a \sim (\gamma t/\eta a)^{1/3}$, we show in figure 3($b$) the collection of our experimental results. All the data collapse on a single curve, even in the initial phase, and they follow the $t^{1/3}$ law at long times ($\gamma t/\eta a > 10^3$). The short-time regime can be associated with the meniscus onset. Our model assumes that the contact angle between the liquid and the wall is $\theta = 0$, fixed by the wetting condition. However, this condition is not fulfilled at $t = 0$ since the liquid is initially horizontal, so the contact angle is $\pi/2$. According to Clanet & Quéré (2002), it takes a time $\tau_m \approx 10^2$–$10^3\ \eta a/\gamma$ to establish the condition $\theta = 0$. This time is compatible with the observations in figure 3($b$). Since it also varies as $\eta a/\gamma$, we understand that the data also collapse in this initial phase.

## 5. A universal law

The law of rise (4.4) is derived without needing the relation $r(x)$ between the tube radius and the distance from the corner. In other words, (4.4) is independent of the actual shape of the corner. To check this strong prediction, we tested three types of corners, namely linear, quadratic and cubic. The linear-type (figure 1$a$) consists of the intersection of two rigid planes with an opening angle $2\alpha$. The distance between the two planes is thus described by $y = \tan\alpha\ x$. We worked with $\alpha = 2.5°$ and $\alpha = 6.5°$ and compared our results with those of Higuera *et al.* (2008), obtained in a more confined geometry ($\alpha = 0.75°$). The quadratic type of equation $y = x^2/D$ is used in figures 1($b$–$d$), 2 and 3. Finally, cubic corners were obtained by pressing two elastic sheets against a solid plane (figure 4$a$ (top view) and figure 4$b$ (side view)). Then, the distance between the elastic walls follows the law $y \approx x^3/L^2$, where $L$ is the length of the sheet.

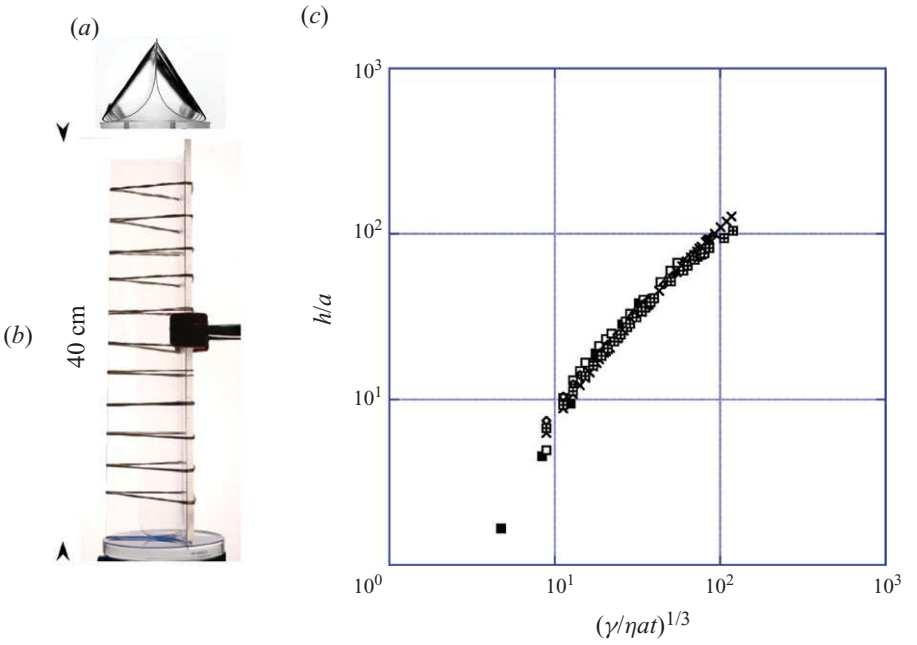


FIGURE 4. (Colour online) (*a*) Top view of a cubic corner of equation $y \simeq x^3/L^2$ created by the compression of elastic mylar sheets. (*b*) Side view of the corner. The horizontal lines are rubber bands that hold the structure. (*c*) Evolution of the reduced height $h/a$ as a function of $(\gamma/\eta at)^{1/3}$ for different corners: (i) linear ($y = \tan\alpha\, x$): ■ data from Higuera *et al.* (2008) ($\alpha = 0.75°$ and silicon oil V460) □ $\alpha = 2.5°$ with a silicon oil V20, ◇ $\alpha = 6.5°$ with a silicon oil V20; (ii) quadratic ($y = x^2/D$): × $D = 30$ mm with a silicon oil V20; (iii) cubic ($y \simeq x^3/L^2$): ⊞ $L = 6$ cm with a silicon oil V20.

These different corners are brought into contact with a silicone oil V20, and the reduced height $h(t)/a$ is measured and plotted in figure 4(*c*) as a function of the non-dimensional time $\gamma\ t/\eta a$. The rise is independent of the corner geometry. Equation (4.4) indeed describes the whole family of rises. Note that the numerical coefficient is found to be of order one.

## 6. Implications for porous media

In complex geometries such as encountered in porous media, one expects to find both closed vessels leading to the Washburn $t^{1/2}$ law, and corners leading to the $t^{1/3}$ law. In this section, we present a device in which these two dynamics appear simultaneously and we discuss their coexistence.

A top view of the channel designed for this experiment is shown in figure 5(*a*). Two elastic sheets (dark grey regions) are clamped together on one side (A) and are pressed against a rigid plate (B) on the other side. This builds up a complex channel (shown in black), in which one finds three corners and a confined region of submillimetric size. Once put vertically in contact with a wetting liquid (again, a silicone oil V20), the rise starts both in the centre of the channel and in the corners. The location of the liquid in the main channel is shown in figure 5(*b*) by solid squares, while open squares indicate the location of the front in one of the corners. In addition, the horizontal crosses show the position of the front in a quadratic corner obtained with solid rods ($D = 30$ mm) with the same silicone oil. It is observed that both capillary rises occur

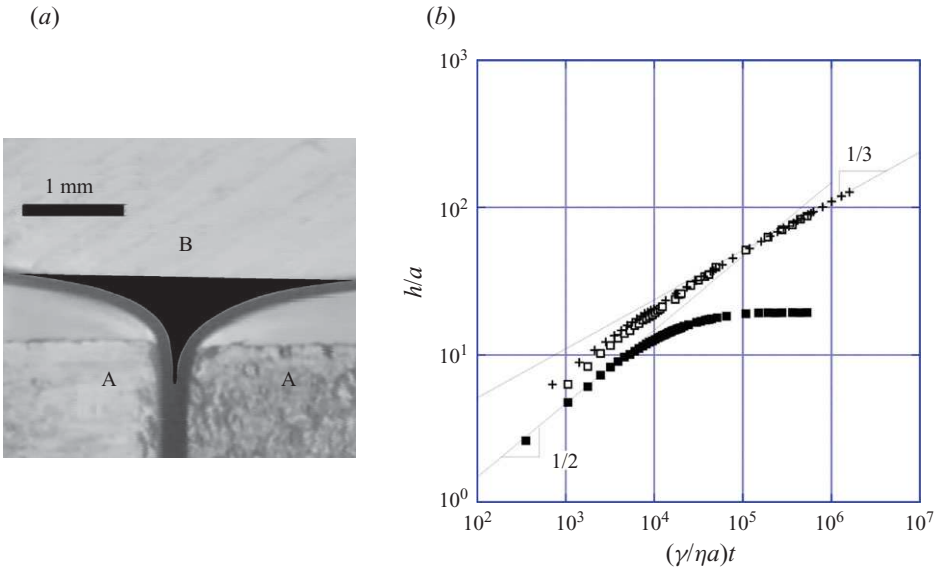


FIGURE 5. (*a*) Device used to study the capillary rise in a complex submillimetric geometry, where a central channel coexists with three corners (black region). (*b*) Location of the liquid front in the centre of the channel (■) and the corner (□). In addition, we show the liquid front in a free quadratic corner (+), with $D = 30\,\text{mm}$ and the same silicone oil V20.

independently of each other. The front in the corner is always the leading front, and apart from the very early stage, it superimposes with the data for an open corner, showing that the filling of the channel does not impact the $t^{1/3}$ dynamics. Conversely, the channel follows the classical Lucas–Washburn law before stopping at a height $h_e \approx 20a$.

One can propose an argument to understand that these features are general and why, in particular, the $t^{1/2}$ law cannot cross the $t^{1/3}$ law at long times. Inside a tube of radius $r$, the wetting liquid moves as $h = \sqrt{\mathscr{D}t}$. Extrapolating the Lucas–Washburn law up to $h = h_e$ enables evaluation of the characteristic time of the rise: $t_e \sim \eta a^4/\gamma r^3$. On the other hand, the time for which we expect a crossover between the two dynamics can be deduced from matching (1.2) and (4.4). We find the same time $t_e$, which implies that a Lucas–Washburn front will experience gravity (and stop) before catching up the meniscus in the corner.

## 7. Conclusion

We have studied the capillary rise of wetting liquids in corners. Using different geometries (linear, quadratic and cubic), we showed that the meniscus rises indefinitely (without saturation), following a universal $t^{1/3}$ law. This result contrasts with most wicking dynamics. The Lucas–Washburn law ($t^{1/2}$), initially derived and observed in a capillary tube, still holds in much more complex geometries (paper, fabric, sand and rough solids). Hence, for each of these geometries, an equivalent radius $r$ can be deduced, which characterizes the wickability of the material. Conversely, there is no such length in a corner which was found to dramatically affect the rise. The absence of characteristic length is also at the origin of the independence of the $t^{1/3}$ law on the corner geometry.

The possible application of this work to capillary rise in trees was discussed with Noel Michele Holbrook during a summer school and with Hervé Cochard at INRA during a seminar. Both discussions were fruitful and have led to ongoing experiments on capillary rise in real stems. May both of them find here the expression of our sincere gratitude.

## REFERENCES

Bico, J. & Qur, D. 2002 Rise of liquids and bubbles in angular capillary tubes. *J. Colloid Interface Sci.* **247**, 162–166.

Boyle 1682 *New Experiments Physico-Mechanical Touching the Spring of the Air and Its Effects.* Oxford H. Hall.

van Brakel, J. & Heertjes, P. M. 1975 Capillary rise in porous media. *Nature* **254**, 585–586.

Caps, H., Cox, S. J., Decauwer, H., Weaire, D. & Vandewalle, N. 2005 Capillary rise in foams under microgravity. *Colloids Surf. Physicochem. Engng Asp.* **261**, 131–134.

Caupin, F., Cole, M., Balibar, S. & Treiner, J. 2008 Absolute limit for the capillary rise of a fluid. *EPL* **82**, 56004.

Clanet, C. & Quéré, D. 2002 Onset of menisci. *J. Fluid Mech.* **460**, 131–149.

Depountis, N., Davies, M. C. R., Harris, C., Burkhart, S., Thorel, L., Rezzoug, A., Knig, D., Merrifield, C. & Craig, W. H. 2001 Centrifuge modelling of capillary rise. *Engng Geol.* **60**, 95–106.

Ferrero, F. 2003 Wettability measurements on plasma treated synthetic fabrics by capillary rise method. *Polym. Test.* **22**, 571–578.

Fries, N. & Dreyer, M. 2008 The transition from inertial to viscous flow in capillary rise. *J. Colloid Interface Sci.* **327**, 125–128.

Galet, L., Patry, S. & Dodds, J. 2010 Determination of the wettability of powders by the Washburn capillary rise method with bed preparation by a centrifugal packing technique. *J. Colloid Interface Sci.* **346**, 470–475.

de Gennes, P. G. 1985 Wetting: statics and dynamics. *Rev. Mod. Phys.* **57**, 827–863.

Hall, C. & Hoff, W. 2007 Rising damp: capillary rise dynamics in walls. *Proc. R. Soc.* A **463**, 1871–1884.

Hardy, W. B. 1922 Historical notes upon surface energy and forces of short range. *Nature* **109**, 375–378.

Higuera, F. J., Medina, A. & Linan, A. 2008 Capillary rise of a liquid between two vertical plates making a small angle. *Phys. Fluids* **20**, 102102.

Hoffman, R. L. 1974 A study of the advancing interface. *J. Colloid Interface Sci.* **50**, 228–241.

Ishino, C., Reyssat, M., Reyssat, E., Okumura, K. & Quéré, D. 2007 Wicking within forest of micro-pillars. *EPL* **79**, 56005.

Jurin, J. 1718 An account of some experiments shown before the Royal Society; with an enquiry into the cause of the ascent and suspension of water in capillary tubes. *Philos. Trans. R. Soc. Lond.* **30**, 739–747.

Karoglou, M., Moropoulou, A., Giakoumaki, A. & Krokida, M. K. 2005 Capillary rise kinetics of some building materials. *J. Colloid Interface Sci.* **284**, 260–264.

Kistler, F. 1993 Hydrodynamics of wetting. *Wettability, Surfactant Science Series* (ed. J. C. Berg), vol. 49. Dekker.

Lago, M. & Araujo, M. 2001 Capillary rise in porous media. *J. Colloid Interface Sci.* **234**, 35–43.

Laplace, P. S. 1878 *Traité de mécanique céleste.* Bachelier Librairie Paris.

Lucas, R. 1918 Rate of capillary ascension of liquids. *Kolloid Z.* **23**, 15.

Marmur, A. 2003 Kinetics of penetration into uniform porous media: testing the equivalent-capillary concept. *Langmuir* **19**, 5956–5959.

Princen, H. M. 1968 Capillary phenomena in assemblies of parallel cylinders. *J. Colloid Interface Sci.* **30**, 69–75.

Princen, H. M. 1969 Capillary phenomena in assemblies of parallel cylinders. *J. Colloid Interface Sci.* **30**, 359–371.

Quéré, D. 1997 Inertial capillarity. *Europhys. Lett*. **39**, 533–538.

Quéré, D., Raphael, E. & Ollitrault, J.-Y. 1999 Rebounds in a capillary tube. *Langmuir* **15**, 3679–3682.

Ramos, A. L. de & Cerro, R. L. 1994 Liquid filament rise in corners of square capillaries: a novel method for the measurement of small contact angles. *Chem. Engng Sci.* **49**, 2395.

Ramrez-Flores, J. C., Bachmann, J. & Marmur, A. 2010 Direct determination of contact angles of model soils in comparison with wettability characterization by capillary rise. *J. Hydrol.* **382**, 10–19.

Siebold, A., Nardin, M., Schultz, J., Walliser, A. & Oppliger, M. 2000 Effect of dynamic contact angle on capillary rise phenomena. *Colloids Surfaces* A **161**, 81–87.

Steen, P. H. 1996 Capillarity and interfacial phenomena, wetting and spreading. In *Research Trends in Fluid Mechanics* (ed. J. L. Lumley, A. Acrivos, L. G. Leal & S. Leibovich), vol. 48. AIP.

Tang, L. H. & Tang, Y. 1994 Capiflary rise in tubes with sharp grooves. *J. Phys.* II **4**, 881–890.

Tanner, L. 1979 The spreading of silicone oil drops on horizontal surfaces. *J. Phys.* D. *Appl. Phys.* **12**, 1473–1484.

Washburn, E. W. 1921 The dynamics of capillary flow. *Phys. Rev.* **17**, 273–283.

Weislogel, M. M. & Lichter, S. 1998 Capillary flow in an interior corner. *J. Fluid Mech.* **373**, 349–378.

Wolf, F. G., dos Santos, L. O. E. & Philippi, P. C. 2010 Capillary rise between parallel plates under dynamic conditions. *J. Colloid Interface Sci.* **344**, 171–179.